Beyond Rectification: Passive Backscattering Modulation

Simon Hemour, Raphael Dauny, Xiaoqiang Gu

Beyond Rectification: Passive Backscattering Modulation

Simon Hemour
IMS Laboratory, CNRS UMR 5218,
Bordeaux INP, University of Bordeaux,
33045 Talence, France
Simon.hemour@u-bordeaux.fr

Raphaël Dauny
IMS Laboratory, CNRS UMR 5218,
Bordeaux INP, University of Bordeaux,
33045 Talence, France
raphael.dauny@u-bordeaux.fr

Xiaoqiang Gu
EEME School,
University of Bristol,
Bristol, UK
sean.gu@bristol.ac.uk

***Abstract*— Wireless Sensor Networks are instrumental to many monitoring systems and control of dynamical systems, allowing real-time and pervasive information collection. However, they are hindered by their dependency on local energy sources, even though their physical transduction principle can be passive. This work proposes an early framework for converting any dc passive sensor into a wireless sensor with passive backscattering modulation capabilities. The operation consists of transforming dc resistance into an RF impedance through the mediation of the nonlinear device of a rectifier.**

Keywords—backscattering, Schottky diodes, rectifier, wireless sensing, zero-power.

I. Introduction

Sensing is a pillar of our technology-oriented societies, linking the real world to cyberspace. In today's context of global change, where every process must be optimized to reduce energy and carbon footprint, sensors are seen as instrumental tools for our civilization's adaptation. Sensors generally gain increased flexibility, scalability, and ease of deployment if they can operate wirelessly. But very few sensors are truly wireless by design. The energy they require to sense and communicate makes them dependent on a wired connection to a power source. Two directions should be followed simultaneously to make sensors free from their energy ties:

The first path is micro-energy local generators, which have been deeply investigated over decades [1]. The second is zero-power communication through backscattering -- a technology initially used for spying purposes [2], where a device communicates by modulating the reflection of an incident radiofrequency (RF) signal back to the transmitter. This modulation can be achieved by varying over time the radar cross section of a scatter, which can be achieved by changing the RF impedance at the output of the antenna's transponder in response to the data to be transmitted. Many backscattering strategies have been proposed [3-5], but all require baseband power to be somehow converted into RF through mixing. Those techniques can be referred to as "active backscattering" and may sometimes be especially power-hungry [6]. For this reason, passive RF transduction sensors (that are more commonly referred to as LC resonators), benefit from important research interests [7], [8]. Thanks to a physical change of inductance or capacitance in time, the reflection coefficient of the resonator changes over time at a given frequency, generating a backscattered signal. However, those sensors are usually custom-built, partly because the resonators need to be fabricated with high quality factors (which can be costly and bulky) to achieve good RF performances. In fact, the massive majority of passive sensors are operating at very low frequencies. Some of them have their resistance changing because of time-varying physical phenomena. This phenomenon can be a variation of a force (switches, resistive force sensor), of strain (strain gauge), of light (photoresistor), etc. With exeption to rare and limited RF implementations [9], those well-performing sensors cannot flow RF current due to their large footprint and/or long connection cable.

This paper introduces a passive circuit that can convert dc resistance variations into RF impedance changes and turn any passive wired sensors into wireless backscattering sensors. The concept is based on "trans-frequency impedance conversion." This work shows that an RF-to-dc power rectifier can also realize dc-to-RF, resistance-to-impedance conversion through the mediation of the nonlinear junction resistance of a Schottky diode.

II. Theoretical Analysis

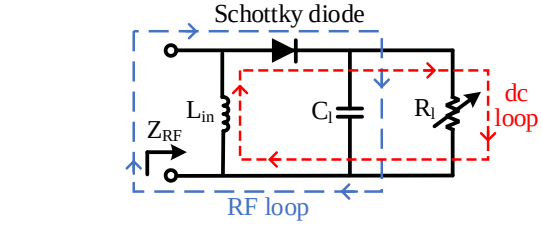

(a)

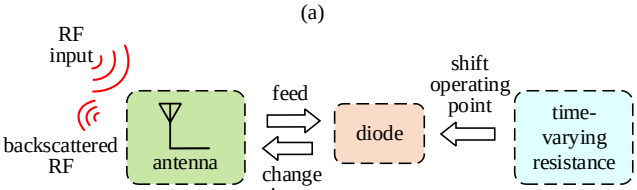

(b)

Fig. 1. (a) Simplified schematic of the passive modulation for backscattering enabled by a Schottky diode and a time-varying resistance; and (b) explanation of how each part of the circuit is interlinked to realize passive modulation.

Figures 1(a) and (b) show how a Schottky diode is utilized to convert dc resistance into RF impedance variations to realize passive modulation. RF input power is received from free space and reaches the Schottky diode for rectification. The rectified dc power can reach the time-varying resistance, which is the R_l in Fig. 1 (a). Due to the changes in time-varying resistance, the operating point of the self-biased diode shifts, leading to the change in RF input impedance. This further influences the RF power level of backscattered signals. The entire interrelated process is illustrated in Fig. 1(b). Two distinct loops, RF and dc, are presented in Fig. 1(a) for better schematic analysis. The load filtering capacitance C_l together with the Schottky diode and receiving antenna forms an RF loop, highlighted using a blue dashed line. The diode acts as an RF power consumer in this RF loop. In comparison, the

inductance L_{in}, the diode and time-varying resistance R_l make a dc loop (the red dashed line in Fig. 1(a)), where the diode is a dc energy generator.

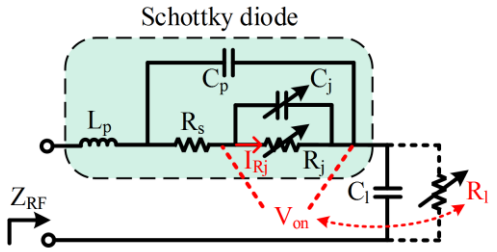

Fig. 2. Shockley diode model included for theoretical analysis at RF frequency. The time-varying load resistance R_l results in the changes in the reflection coefficient of this design.

The components involved in the RF loop are shown in Fig. 2. The Shockley diode model, which is an effective way to characterize Schottky diodes, is adopted for theoretical analysis [10]. C_j and R_j are nonlinear junction capacitance and nonlinear junction resistance, respectively. R_s is the series resistance. L_p and C_p are packaging parasitics. Let us start by assuming V_{on} and I_{R_j} are the voltage across and current passing the nonlinear junction resistance R_j of the Schottky diode. Since R_l is short-circuited at RF frequency, but it influences both V_{on} and I_{R_j}, R_l is connected to the circuit with a dashed line. Then, the voltage across the series resistance of the diode R_s is:

$$V_{R_s} = \left(V_{on} \cdot j\omega C_j + I_{R_j}\right) \cdot R_s \tag{1}$$

where $\omega = 2\pi f$ is the angular frequency. The current entering the diode is:

$$I_{in} = (V_{on} + V_{R_s}) \cdot j\omega C_p + V_{on} \cdot j\omega C_j + I_{R_j} \tag{2}$$

The voltage at the RF input can be obtained by:

$$V_{in} = V_{on} + V_{R_s} + I_{in} \cdot j\omega L_p \tag{3}$$

So, the input impedance can be obtained as:

$$Z_{RF} = \frac{V_{in}}{I_{in}} \tag{4}$$

Assuming the characteristic impedance is standard 50 Ω, the reflection coefficient Γ can be obtained by:

$$\Gamma = \frac{Z_{RF}-50}{Z_{RF}+50} \tag{5}$$

Since V_{on} and I_{R_j} are associated with R_l, Z_{in}, and Γ are also dependent on R_l. With the theoretical model used for rectification analysis [11], [12], the relationship between R_l and Z_{in} can be obtained analytically. An SMS7630 Schottky diode is used for this analysis. Operating frequency is 1 GHz, and input power is set at −30 dBm. To compensate for the nonlinear junction capacitance C_j and packaging capacitance C_p, an 83.3-nH inductor is put in series with the SMS7630 diode. Fig. 3(a) shows the Γ distribution on a Smith chart while R_l changes from 1 Ω to 100 kΩ. The results without the matching inductor are also included for comparison. Clearly, the curve can be shifted to the middle of the Smith chart with the matching inductor. Furthermore, R_l can have a significant influence on Γ. If R_l varies in a sine waveform from 0 Ω to 200 kΩ with a frequency $1/2\pi$ Hz, as shown in Fig. 3(b) top, the corresponding S11 in dB and the fraction of power backscattered by the circuit are demonstrated in Fig. 3(b) middle and bottom, respectively. From Fig. 3(b) middle, the overall matching results are acceptable with −30-dBm RF input, when R_l varies from 0 Ω to 200 kΩ. When R_l is high (200 kΩ), the S11 is about –6.4 dB, which means that about 22.8 % power is backscattered. This is highlighted by line ①. Then, with R_l decreasing to about 8050 Ω, S11 would reach its valley, –23.7 dB. Almost no power is backscattered in this case, corresponding to line ②. If R_l continue to reduce and close to 0 Ω, S11 bounces to –8.6 dB, and 13.7 % RF input power is backscattered, which is indicated by line ③. When R_l increases from 0 Ω to 8050 Ω (line ④), this rectifier will have the same performance as explained at line ②.

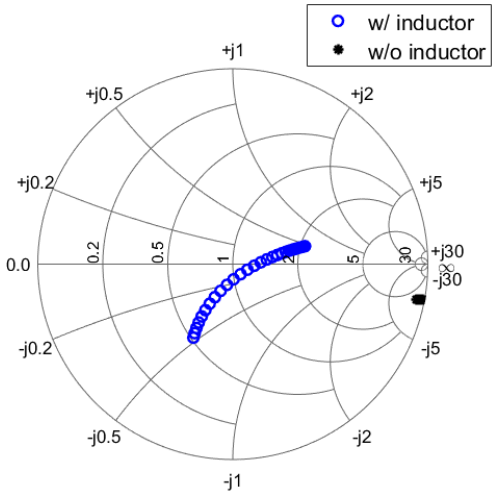

(a)

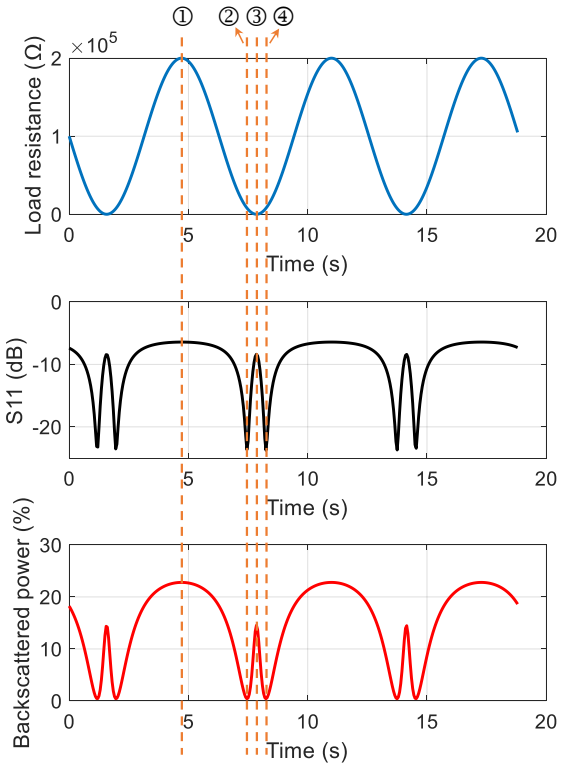

(b)

Fig. 3. (a) Reflection coefficient distribution when R_l changes from 1 Ω to 100 kΩ. (b) When R_l varies in a sine waveform (0 Ω to 200 kΩ) (top), the S11 of the circuit (middle) and the fraction of RF input power backscattered by the circuit (bottom) change accordingly.

An important parameter that determines the power of the backscattered signal is differential radar cross-section (RCS). It can be calculated by [13]:

$$\sigma_d = \frac{\lambda^2 G_r^2}{4\pi} \frac{|\Delta\Gamma|^2}{4} \tag{6}$$

where λ is wavelength (0.3 m) and G_r is rectifier antenna gain (assuming to be 1). $|\Delta\Gamma|$ is the complex reflection coefficient differences of two states due to R_l variations. Fig. 4 (a) shows the reflection coefficient differences with respect to the initial value ($R_l = 0\ \Omega$) when R_l changes from 0 Ω to 100 kΩ. With the increase of R_l, $|\Delta\Gamma|$ becomes larger, which is consistent with the observation in Fig. 3(a).

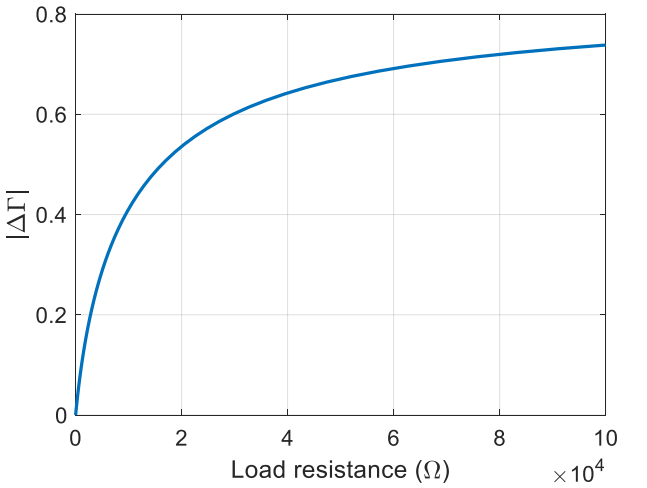

(a)

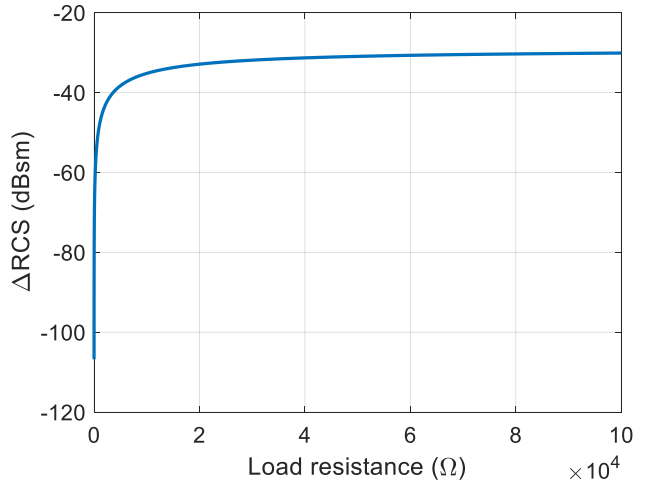

(b)

Fig. 4. (a) Reflection coefficient differences with respect to its initial value $|\Delta\Gamma|$ and (b) differential radar cross-section σ_d as a function of load resistance R_l in a range of 0 Ω to 100 kΩ.

Furthermore, the read range can be estimated based on the evaluation of differential or delta RCS information in (6). The read range in non-isolated channels can be calculated by [14]:

$$d \leq \sqrt[4]{\frac{P_t G_t G_r \lambda^2 \sigma_d}{(4\pi)^3 P_{rr\,min}}} \tag{7}$$

in which P_t and G_t are transmitted power and transmitting antenna gain, respectively. $P_{rr\,min}$ is the receiving reader sensitivity, which is the minimal differential backscattered power that can be detected. As shown in Fig. 5(a), assuming the transmitter is sending an effective isotropic radiated power of $P_t G_t$ = 36 dBm, G_r = 1 (0 dB), and $P_{rr\,min}$ = −60 dBm, the read range of this proposed backscatter due to rectifier load change can be evaluated, as seen in Fig. 5(b). The read range continues to increase with a larger load resistance, which is due to a larger delta RCS, as shown in Fig. 4(a).

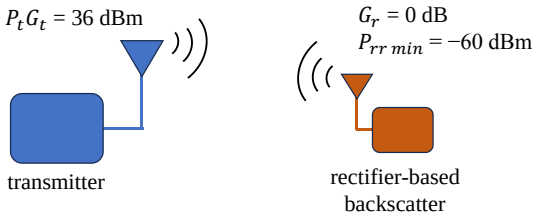

(a)

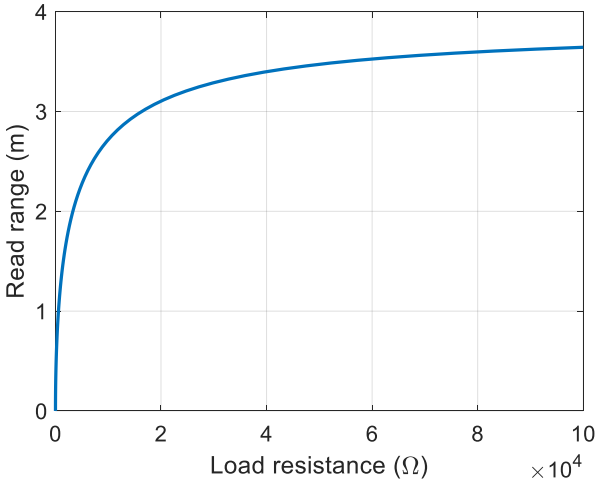

(b)

Fig. 5. (a) Set-up diagram of read range evaluation and (b) calculated read range of proposed rectifier-based backscatter.

III. Measurements

A proof-of-concept trans-frequency impedance converter circuit is fabricated with a Skyworks SMS7030-079LF Schottky diode (typical video resistance = 5 kΩ), and a Johanson Technology R07S-series, low ESR capacitor multi-layer high-Q capacitor (30 pF, ±5 %, resonant frequency = 1.8 GHz). To avoid dc current flowing through the 50-Ω internal resistance of the Vector Nectwork Analyzer (VNA), a parallel coil-based matching is used. The diode circuit is L-matched with a coilcraft 0807SQ-10N square air core inductors in parallel (10.2 nH, ±5 %, self resonant frequency = 4 GHz, not shown in the figure) followed by a coilcraft 0603CS-68N high temperature ceramic chip inductors (68 nH, ±5 %, self resonant frequency = 1.7 GHz) in series.

VNA S11 measurements for the fabricated circuit are shown in Fig. 6 for two extreme cases of resistive sensor loading. When the circuit is excited with a 1-μW power at 947 MHz, a dc resistance of 100 MΩ yields a reflection coefficient of about 15 % whereas a dc resistance of 0 Ω yields a reflection coefficient of 55 %, resulting in a ΔΓ of approx. 40 % (and an amplitude modulation depth of 57% for the backscattered signal). Considering the same conditions detailed earlier, this would yield a read range above 2.5 m.

To backscatter maximum power, the trans-frequency impedance conversion ΔΓ must be large, translating into large RF impedance variation. This means that the two dc operating points should be as far as possible on the exponential-shaped I-V curve of the Schottky diode. While one of them corresponds to zero bias current, it is clear that the other operating corresponds to maximum self-bias current, which implies that it should be used both a minimum dc resistance, and optimum RF matching condition.

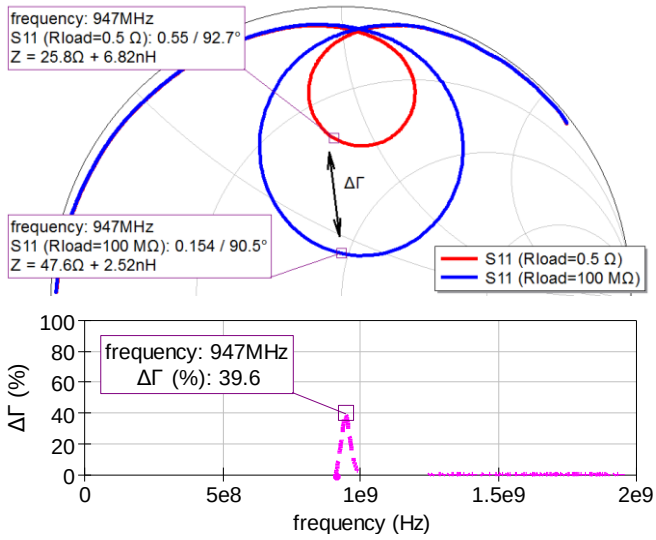

Fig. 6. Reflection coefficient of the trans-frequency impedance converter for two extreme dc loads (red and blue solid lines). The variation of reflection coefficient ΔΓ is plotted in a pink dashed line.

IV. Conclusion

This work shows a passive modulation circuit requiring no dc power to operate. Thanks to its inner self-biased mechanism, It can convert dc resistance variations ΔR into RF impedance changes ΔZ, and turn any passive wired resistive sensors into a wireless backscattering sensor through the "transformation sensitivity" (ΔZ/ΔR), which depends on many factors, such as the current responsivity of the diode, the dc self-biasing current and the RF matching network. This method is especially suitable for getting wireless access to the state of an analog resistive sensor across the skin (bioelectronics sensor) or any industrial barrier (solid concrete for structural health monitoring, thermal insulation for non-destructive control).

Acknowledgement

The author would like to acknowledge the funding of R.D. from the grants ANR-21-CE19-0015-01, and UB RRI BEST.

Reference

[1] K. Niotaki *et al.*, "RF Energy Harvesting and Wireless Power Transfer for Energy Autonomous Wireless Devices and RFIDs," *IEEE Journal of Microwaves*, vol. 3, no. 2, pp. 763-782, 2023, doi: 10.1109/JMW.2023.3255581.

[2] P. Nikitin, "Leon Theremin (Lev Termen)," *IEEE Antennas and Propagation Magazine*, vol. 54, no. 5, pp. 252-257, 2012, doi: 10.1109/MAP.2012.6348173.

[3] B. Kellogg, A. Parks, S. Gollakota, J. R. Smith, and D. Wetherall, "Wi-Fi backscatter: Internet connectivity for RF-powered devices," in *Proceedings of the 2014 ACM Conference on SIGCOMM*, 2014, pp. 607-618.

[4] R. Correia, N. B. Carvalho, and S. Kawasaki, "Continuously Power Delivering for Passive Backscatter Wireless Sensor Networks," *IEEE Trans. Microw. Theory Tech.*, vol. 64, no. 11, pp. 3723-3731, 2016, doi: 10.1109/TMTT.2016.2603985.

[5] X. Tang, G. Xie, and Y. Cui, "Self-Sustainable Long-Range Backscattering Communication Using RF Energy Harvesting," *IEEE Internet of Things Journal*, vol. 8, no. 17, pp. 13737-13749, 2021, doi: 10.1109/JIOT.2021.3067948.

[6] D. Belo *et al.*, "IQ Impedance Modulator Front-End for Low-Power LoRa Backscattering Devices," *IEEE Trans. Microw. Theory Tech.*, vol. 67, no. 12, pp. 5307-5314, 2019, doi: 10.1109/TMTT.2019.2941854.

[7] Q. A. Huang, L. Dong, and L. F. Wang, "LC Passive Wireless Sensors Toward a Wireless Sensing Platform: Status, Prospects, and Challenges," *Journal of Microelectromechanical Systems*, vol. 25, no. 5, pp. 822-841, 2016, doi: 10.1109/JMEMS.2016.2602298.

[8] K. S. V. Idhaiam, P. D. Pozo, K. Sabolsky, E. M. Sabolsky, K. A. Sierros, and D. S. Reynolds, "All-Ceramic LC Resonator for Chipless Temperature Sensing Within High Temperature Systems," *IEEE Sensors Journal*, vol. 21, no. 18, pp. 19771-19779, 2021, doi: 10.1109/JSEN.2021.3094406.

[9] H. Ribeiro, S. Hemour, and N. B. Carvalho, "Fully Passive Modulation Technique for SWIPT Scenarios," in *2023 IEEE/MTT-S International Microwave Symposium - IMS 2023*, 11-16 June 2023 2023, pp. 999-1002, doi: 10.1109/IMS37964.2023.10188111.

[10] X. Gu, S. Hemour, and K. Wu, "Far-Field Wireless Power Harvesting: Nonlinear Modeling, Rectenna Design, and Emerging Applications," *Proc. IEEE*, vol. 110, no. 1, pp. 56-73, 2022, doi: 10.1109/JPROC.2021.3127930.

[11] X. Gu, S. Hemour, L. Guo, and K. Wu, "Integrated Cooperative Ambient Power Harvester Collecting Ubiquitous Radio Frequency and Kinetic Energy," *IEEE Trans. Microw. Theory Tech.*, vol. 66, no. 9, pp. 4178-4190, 2018.

[12] X. Gu, L. Guo, S. Hemour, and K. Wu, "Optimum Temperatures for Enhanced Power Conversion Efficiency (PCE) of Zero-Bias Diode-Based Rectifiers," *IEEE Transactions on Microwave Theory Techniques*, 2020.

[13] A. Voisin, A. Dumas, N. Barbot, and S. Tedjini, "Differential RCS of Multi-State Transponder," in *2022 Wireless Power Week (WPW)*, 5-8 July 2022 2022, pp. 195-198, doi: 10.1109/WPW54272.2022.9853941.

[14] N. Barbot, O. Rance, and E. Perret, "Classical RFID Versus Chipless RFID Read Range: Is Linearity a Friend or a Foe?," *IEEE Trans. Microw. Theory Tech.*, vol. 69, no. 9, pp. 4199-4208, 2021, doi: 10.1109/TMTT.2021.3077019.